JACS
JOURNAL OF THE AMERICAN CHEMICAL SOCIETY
pubs.acs.org/JACS
Article

Tunable Symmetry-Breaking-Induced Dual Functions in Stable and Photoswitched Single-Molecule Junctions

Na Xin,[†] Chen Hu,[†] Hassan Al Sabea,[†] Miao Zhang,[†] Chenguang Zhou,[†] Linan Meng, Chuancheng Jia, Yao Gong, Yu Li, Guojun Ke, Xiaoyan He, Pramila Selvanathan, Lucie Norel, Mark A. Ratner, Zhirong Liu,* Shengxiong Xiao,* Stéphane Rigaut,* Hong Guo,* and Xuefeng Guo*

Cite This: *J. Am. Chem. Soc.* 2021, 143, 20811−20817

Read Online

ACCESS | Metrics & More | Article Recommendations | Supporting Information

ABSTRACT: The aim of molecular electronics is to miniaturize active electronic devices and ultimately construct single-molecule nanocircuits using molecules with diverse structures featuring various functions, which is extremely challenging. Here, we realize a gate-controlled rectifying function (the on/off ratio reaches ∼60) and a high-performance field effect (maximum on/off ratio >100) simultaneously in an initially symmetric single-molecule photoswitch comprising a dinuclear ruthenium-diarylethene (Ru-DAE) complex sandwiched covalently between graphene electrodes. Both experimental and theoretical results consistently demonstrate that the initially degenerated frontier molecular orbitals localized at each Ru fragment in the open-ring Ru-DAE molecule can be tuned separately and shift asymmetrically under gate electric fields. This symmetric orbital shifting (AOS) lifts the degeneracy and breaks the molecular symmetry, which is not only essential to achieve a diode-like behavior with tunable rectification ratio and controlled polarity, but also enhances the field-effect on/off ratio at the rectification direction. In addition, this gate-controlled symmetry-breaking effect can be switched on/off by isomerizing the DAE unit between its open-ring and closed-ring forms with light stimulus. This new scheme offers a general and efficient strategy to build high-performance multifunctional molecular nanocircuits.

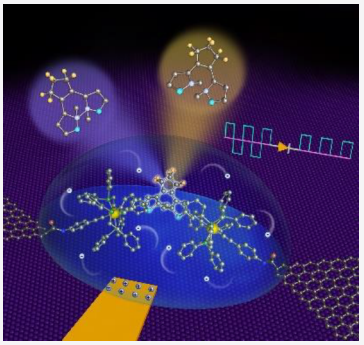

INTRODUCTION

Single-molecule electronics, in which one or a few molecules are used to construct an electronic component, is regarded as a complementary technological option to conventional Si-based microelectronics and thus has aroused tremendous interest from researchers with interdisciplinary backgrounds.[1−4] Until now, various functionalities have been realized in both single-molecule junctions and large-area molecular junctions, including switches,[5,6] memristors,[7,8] rectifiers,[9,10] field-effect transistors (FETs),[11,12] and so on. To this end, the fabrication of multifunctional molecular nanocircuits using devices such as single-molecule FETs and single-molecule rectifiers is considered to be a crucial step toward bringing these devices into daily life,[13] as illustrated in the international semiconductor industry roadmap released in 2016, rather than simply continue to follow Moore's law.[14]

FETs are one of the most elementary components in electronic circuits, and molecular-scale FETs combined with other functions, like rectification and switch, promise potential applications in information technology.[15] The typical working mechanism for single-molecule FETs is to tune the molecular orbital energy levels relative to the bias voltage window, however, most of the reported on/off ratio of single-molecule FETs were rather moderate (∼10).[11,16−18] Recently, anti-resonance states were utilized to suppress the off-state conductance, achieving on/off ratios of around 2 orders of magnitude.[19,20] Different inspiring approaches are still in great need to improve the performance of single-molecule FETs. To integrate additional functions into single-molecule FETs, a general idea is to control classic single-molecule diodes with gate, which was proved not so effective in modulating either the rectification ratio or the FET on/off ratio.[21,22] The formidable challenge is that the asymmetrically electronic feature through a molecular junction is difficult to change in a specific molecular diode. Moreover, to change the rectification ratio of a single-molecule diode *in situ* is of significance as it can save tedious chemical synthesis that have been commonly used to modulate the asymmetry of the molecular kernel. Here, we demonstrate an unprecedented gate electric-field-induced symmetry-breaking effect with photocontrollability in an initially symmetric single-molecule junction, which simultaneously leads to a tunable rectifying behavior and good FET performances, thus realizing multiple functions within one molecular junction.

Received: August 25, 2021
Published: November 30, 2021

https://doi.org/10.1021/jacs.1c08997
J. Am. Chem. Soc. 2021, 143, 20811−20817

RESULTS AND DISCUSSION

Diarylethene (DAE) derivatives have been intensively used to construct molecular switches for more than two decades because they can undergo reversible and rapid photo-transformations between open-ring (*o*) and closed-ring (*c*) isomers with superior thermal stability and fatigue resistance.[23,24] Here, we designed a dinuclear Ru-DAE complex containing two Ru fragments $[H_2N-p-C_6H_4-C{\equiv}C-(dppe)_2Ru]^+$ (dppe = 1,2-bis(bipehenylphosphino)ethane) at two mirror-symmetric α-positions of the two thiophene rings (Figure 1a and Scheme S1). As shown in Figure 1b, quantum

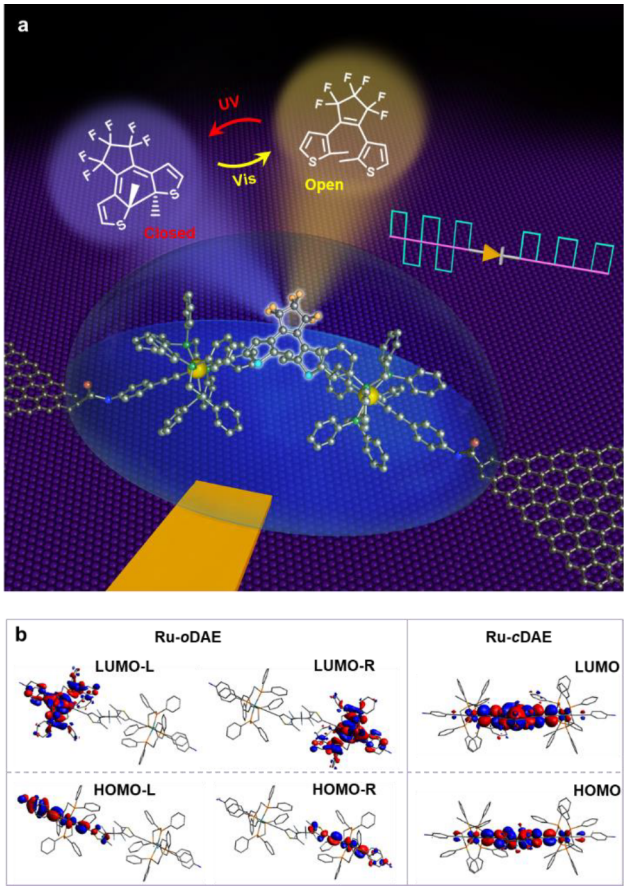

Figure 1. Device structure of a graphene-Ru-DAE-graphene single-molecule junction and associated FMO diagrams. (a) Schematic representation of a graphene-Ru-DAE-graphene single-molecule transistor with ionic liquid gate dielectric that highlights the light-stimulated DAE isomerization between the closed-ring and open-ring forms (Ru-*c*DAE and Ru-*o*DAE). (b) FMO diagrams for Ru-*o*DAE and Ru-*c*DAE, showing distinct differences.

chemistry calculations based on the density functional theory (DFT) for the gas-phase isolated Ru-*c*DAE and Ru-*o*DAE indicate that the two forms have different geometric configurations of their Ru nuclei and frontier molecular orbitals (FMOs). In Ru-*c*DAE, the Ru nuclei are in the same plane as DAE, with the FMOs delocalized symmetrically throughout the entire molecular backbone bridged by strong conjugation. In contrast, in Ru-*o*DAE, the two thiophene rings are in C_2 symmetry (antiparallel conformation) and two Ru nuclei are located above/below the central plane, because of the broken orbital conjugation and the steric repulsion between two Ru fragments.[25] Correspondingly, paired nearly degenerate FMOs are localized on each side of the molecular backbone: the localized HOMO-L/R and LUMO-L/R (Figure 1b). Such unique orbital localization feature provides the high possibility of tuning their FMOs either collectively or separately, thus laying a foundation for the novel electronic properties described below.

The device fabrication process of graphene-Ru-DAE-graphene single-molecule junctions (SMJs) is described in the Supporting Information. We first investigated the photo-switching property of the Ru-DAE-reconnected SMJs, which demonstrated reproducible conductance switching (Figures 2a,

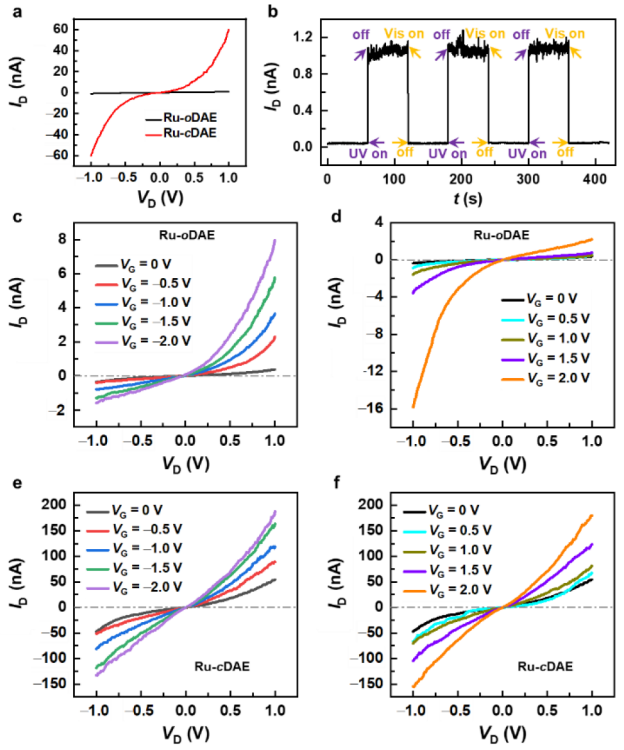

Figure 2. Reversible photoswitching and field-effect characteristics of an individual Ru-DAE SMJ. (a) Current−voltage (I_D-V_D) curves of individual Ru-DAEs in open-ring (dark) and closed-ring (red) forms at V_G = 0 V. (b) Real-time measurement of the current passing through a Ru-DAE molecule that switches reversibly back-and-forth between its closed-ring and open-ring forms upon exposure to ultraviolet (UV: 365 nm) and visible (Vis: 650 nm) lights, respectively. V_D = 0.1 V and V_G = 0 V. (c, d) Representative gate-dependent I_D-V_D characteristics for the open-ring form. (e, f) Representative gate-dependent I_D-V_D for the closed-ring form.

b and Figure S11) under alternating visible/ultraviolet (Vis/UV) light irradiation in vacuum at room temperature, consistent with previous studies.[26−32] This reversibility was confirmed further by time-dependent UV−vis absorption experiments (Figure S4), nuclear magnetic resonance (NMR) investigations (Figures S2, S5, and S6) on a reference compound mimicking the junction chemical structure (Scheme S4) and theoretical transmission calculations (Figure S23).

Using an ionic liquid as gate dielectric (with a ∼7.5 Å thick electrical double layer, Figures S9 and S10) which has been demonstrated as an effective method to tune molecular orbital energies,[33,34] we investigated the FET behavior of the Ru-DAE SMJs and their tunability. As a result, it was found that the Ru-

https://doi.org/10.1021/jacs.1c08997
J. Am. Chem. Soc. 2021, 143, 20811−20817

DAE SMJs (both Ru-*o*DAE and Ru-*c*DAE) exhibited obvious gate-dependent current−voltage (I_D−V_D) characteristics (Figures 2c, d for Ru-*o*DAE; Figure 2e, f for Ru-*c*DAE; Figures S12−S14). The current passing through these junctions increases as the gate voltage (V_G) becomes increasingly positive or negative, which is indicative of ambipolar characteristics. Interestingly, we also found that the Ru-*o*DAE output characteristics under gate electric field show clear asymmetric conductance behavior with bias dependence (Figures S12 and S16−S18) and the rectification directions under the positive and negative gate electric fields are opposite (Figure 2c, d; Figures S13 and S14), though the I−V plots at the zero-gate voltage are nearly symmetrical (Figure S15). Specifically, we calculated the rectification ratio (RR, I_{on}/I_{off}) at each bias voltage under different gate voltages and found that the RR increases with increasing $|V_G|$ (Figures 3a and Figure S19a). In contrast, when we performed a similar analysis for Ru-*c*DAE SMJs, the I_D−V_D curves under different gate voltages were nearly symmetrical and RRs at each bias were close to unity, independent of the gate voltage (Figure S19b). Note also that the gate-dependent I_D−V_D curves of both Ru-*o*DAE and Ru-*c*DAE (Figure 2 and Figure S13) were measured *in situ* before and after device UV irradiation. On the basis of this fact, we concluded that the gate-controlled rectifying behavior in the Ru-*o*DAE SMJs is induced by the gate electric field, excluding other potential artifacts that possibly result from device-to-device variations at the molecule−electrode interfaces.

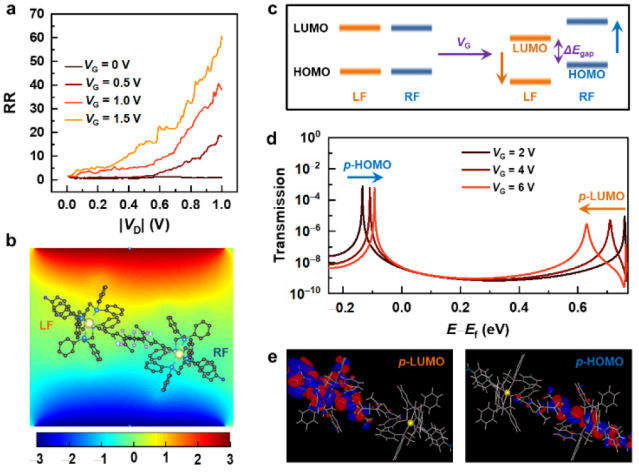

Figure 3. Rectification and theoretical model of Ru-*o*DAE SMJs. (a) Gate-dependent rectification ratio for another Ru-*o*DAE SMJ (Device 2). For the corresponding I_D−V_D characteristics of this device, see Figure S11. (b) Gate-induced electric potential distributions in the central region of Ru-*o*DAE SMJs at V_G = 6 V obtained through NEGF-DFT simulations. The scaling unit of the color bar is eV. For an intuitive demonstration, the molecule positions are also marked and plotted. LF and RF denote the left Ru fragment and the right Ru fragment, respectively. (c) Schematic illustration of the AOS processes of the two Ru fragments under V_G. The local FMOs of the LF and RF are coded using orange and blue colors. Orange and blue arrows indicate the orbital-shifting tendencies of LF and RF. (d) Transmission spectra of Ru-*o*DAE SMJs for different V_G values. E_f is the Fermi level of the graphene electrodes. (e) Real-space distributions of scattering states of *p*-HOMO and *p*-LUMO of Ru-*o*DAE SMJs.

Statistical analysis of RR at ±1.0 V bias (V_G = ± 2.0 V) among different Ru-*o*DAE devices indicated the high rectification performance (Table S1) with mean and maximum values as ∼19 and ∼61, respectively. In addition, the FET property at the rectification polarity exhibited an exceptional behavior: the mean on/off ratio is ∼59 with the maximum value as high as ∼144 (Table S2). For the reverse bias range where the off-state of rectification appears, the FET behavior is moderate with an on/off ratio of <10.

As the open-ring DAE unit works as a weakly conjugated bridge to connect the two Ru fragments, their localized FMOs are separated well, meaning that each Ru fragment can be tuned and manipulated independently. At V_G = 0 V, the molecular system is symmetrical and the perturbed (*p*)-FMOs of the left fragment (LF) and the right fragment (RF) are degenerate. When V_G is applied, the Ru fragments at each side in Ru-*o*DAE are gated asymmetrically because they are located at different potential positions in the gate electric field (Figures 3b and Figure S24). This asymmetric gating effect breaks the energy degeneracy and causes asymmetric orbital shifting (AOS) of the two Ru fragments (Figure 3c, assuming the situation as what is shown in Figure 3b), resulting in an electronic profile close in spirit to the D-σ-A scheme in the original Aviram−Ratner rectification paper.[35,36] The physics of this process is captured further by calculating the quantum charge-transport properties of the molecular junction in combination with graphene electrodes using the DFT within the nonequilibrium Green's function (NEGF) technique (calculation details are presented in the Supporting Information). As shown in Figure 3d, the induced asymmetry becomes larger with increasing V_G: The *p*-HOMO shifts upward and the *p*-LUMO shifts downward, thus the energy gap between them (ΔE_{gap}) getting smaller, as well as that between *p*-FMOs and the graphene Fermi level. According to the energy-dependent Landauer formalism of quantum transport, the energy gap between *p*-FMOs and the Fermi level of the electrodes plays an essential role in the current under low bias voltages: A smaller gap size allows more electrons to enter the Fermi window within the applied bias range. Consequently, we conclude that V_G can enhance the charge transport, thus improving the FET behavior observed above.

The wave function calculations of the transport scattering states shown in Figure 3e demonstrate that *p*-LUMO and *p*-HOMO are separately contributed from each local fragment (LF and RF, respectively), which further verifies the AOS process shown in Figure 3c, d. Such AOS is essential to the intrinsic molecular rectification mechanism: Positive and negative biases have opposite effects on the transmission gap (level misalignment), thus leading to significantly different transport processes (mechanism details can be seen in Figure S26). This working principle is similar to those previously reported.[22,37] Note here that we demonstrate the physical mechanism by considering only one polarity for V_G in the discussion above. Obviously, if the direction (or polarity) of V_G is reversed, the AOS process and rectification effect will then be opposites to the original effects, which is consistent with the experimental observations shown in Figures 2c, d (Figures S13 and S14). Additionally, the relative spatial position of LF and RF is stochastic in real device systems: LF is above or below the RF. In the case where LF is below RF, the rectification direction should be opposite to that shown in Figures 2c, d; this has also been observed experimentally (Figures S13 and S16−S18). These Ru-*o*DAE SMJs represent an intrinsic molecular rectifier established in an initially symmetrical single-molecule junction including source/drain electrodes of

https://doi.org/10.1021/jacs.1c08997
J. Am. Chem. Soc. 2021, 143, 20811−20817

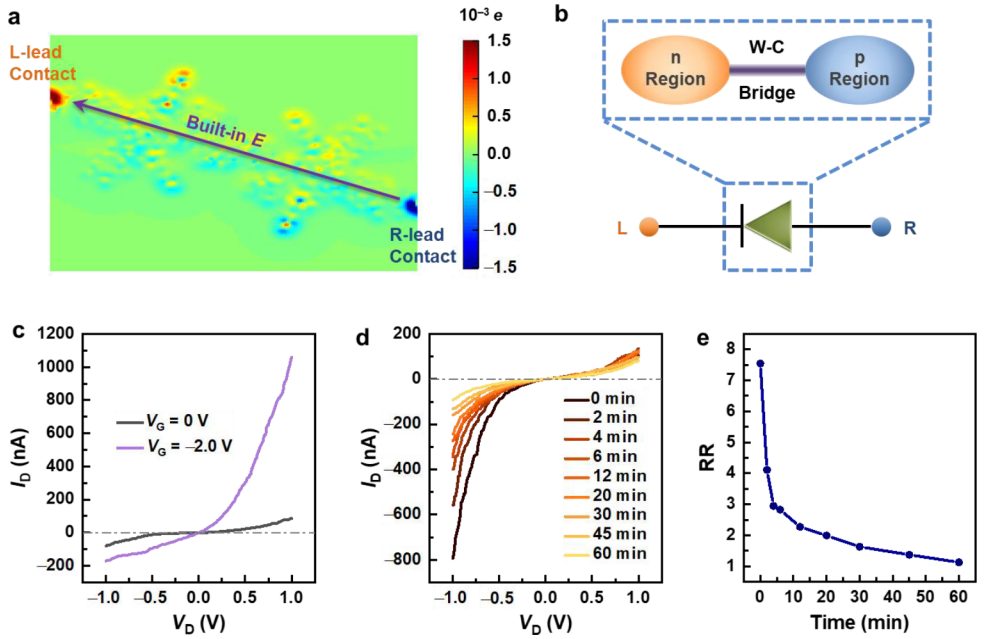

Figure 4. Decay process of rectification after the gate voltage is offloaded. (a) Differences in the electron density distribution within the Ru-*o*DAE backbone between V_G = 6 V and V_G = 0 V, obtained through NEGF−DFT simulations. (b) Schematic illustration of the rectification mechanism at the moment when V_G is offloaded. A *p*−*n* junction is formed and connected via a weakly conjugated (W−C) bridge. (c) I_D−V_D characteristics of another Ru-*o*DAE SMJ (Device 3) before and after V_G is loaded. (d) Time-dependent I_D−V_D characteristics of the Ru-*o*DAE after V_G is offloaded. (e) Rectification ratio decay with time. The charge transport behavior finally restored to its original state before V_G is loaded.

the similar size; it differs from previous reported cases in which asymmetry was induced using extrinsic methods, including chemical strategies such as donor−acceptor structures,[21,22,38,39] electrode materials,[40] anchoring/spacer groups,[36,41,42] and molecular intercalation[43] and physical methods, e.g. ,geometric asymmetry between both electrodes of the same material,[9,37] where asymmetric electrostatic environments were introduced at the molecule−electrode interface in the presence of polar solvents, thus inducing the rectifying behavior. In addition, a novel rectification mechanism has been reported based on self-assembled monolayers,[10] where the electroactive ferrocenyl moiety was typically placed asymmetrically between a platinum surface and an EGaIn tip by inserting a long alkyl chain on the platinum side and Coulombic interaction induced an increase in the number of conducting molecules under forward biases, thus realizing RRs exceeding 1×10^5.

Essentially unlike the open-ring isomer, there exist strong conjugation and orbital delocalization between two fragments in Ru-*c*DAE, making it difficult to tune LF and RF separately. As shown in Figure S25, there is no obvious AOS under different gate voltages, which implies that the symmetry is maintained throughout the molecular backbone with V_G, i.e., no rectification effect appears (Figures 2e, f and Figure S13). Therefore, the application of different gate voltages induces only the general FET effect. For the moderate FET performances, it should be attributed to the delocalized electronic structure, which contributes to relatively large off-state current. Furthermore, we designed and synthesized a control molecule (see Scheme S3) with the similar structure to Ru-DAE, in which the DAE unit is replaced by a phenyl ring and the two Ru fragments are placed at each para-position, respectively. No obvious rectifying effect appears in the gate-dependent I_D−V_D characteristics of SMJs reconnected by this control molecule (Figure S22), which clearly proves that it is the conjugation difference that dominates the distinct gate-dependent behaviors between open/closed-ring isomers. Note that (1) there is a C_2 symmetry in the open form (2 antiparallel conformations), which has a helicoidal chirality with 2 enantiomers with the P or M helicity, whereas in the closed form, there is also a C_2 symmetry with 2 enantiomers (with 2 chiral carbons, one methyl up and one methyl down with respect to the diarylethene plane); (2) there is a tiny length change in molecular length (∼0.14 Å) between the closed-ring (∼31.15 Å long) and open-ring (∼31.29 Å long) forms; (3) the linkage amide modes might be asymmetric under an applied field.[44,45] What is left unclear is that in addition to the symmetry breaking mechanism, whether the rectification synergistically originates from the chirality, the length change (which might be influenced by electrical fields), the asymmetry of amide bonds under electrical fields or another associative mechanism.

The asymmetric gating effect in the Ru-*o*DAE system can also induce a high degree of charge transfer between LF and RF. In Figure 4a and Figure S27, we found that charge transfer produces a built-in polarization electric field from right to left (opposite to the external gate field). When the gate is loaded, the external gate field is stronger than the built-in polarization field, thus dominating the effect. When the gate (i.e., the external field) is offloaded, the gate-induced charge transfer cannot disappear rapidly because the weakly conjugated bridge suppresses free movement of electrons and charges. The built-in field will thus start to dominate and form a *p*−*n* junction system, which leads to another rectification process (Figure 4b). This new type of rectification shows the opposite polarity to the rectification effect when V_G is loaded (Figure 4c, d; Figures S20 and S21). Additionally, this rectification is sensitive to the charge retransfer process and thus expected to decay over time. After sufficient time, this off-loaded rectification phenomenon will disappear, which is consistent with the experimental observations shown in Figures 4d, e. The

https://doi.org/10.1021/jacs.1c08997
J. Am. Chem. Soc. 2021, 143, 20811−20817

rectification ratio decays with time at a decreasing rate, but not in a single exponent way. Note that the decaying time scale qualitatively agrees well with other studies on intramolecular electron transfer in cobalt−iron Prussian blue analogues.[46−48] This rectification decay process after the gate voltage is offloaded further verifies the AOS scheme as discussed above. The detailed study of the charge relaxation process is out of the scope of this work and will be the subject of the next report.

CONCLUSIONS

In this work, we achieved *in situ* controllable multifunctional single-molecule devices with photoswitching, rectification and FET performances. The key is that gate voltage can be used to induce the AOS process that leads to the corresponding symmetry-breaking effect in an initially symmetric molecule, thus realizing the rectification function with practical features: an on/off switch, polarity control, and magnitude modulation. This AOS process also enhances the FET performances with the maximum conductance variation larger than 2 orders of magnitude. Rational molecular design with various structures and functions offers a wealth of possibilities for constructing high-performance multifunctional molecular integrated circuits, paving the way toward real applications.

ASSOCIATED CONTENT

Supporting Information

The Supporting Information is available free of charge at https://pubs.acs.org/doi/10.1021/jacs.1c08997.

Molecular synthesis; isomerization studies in solution; device fabrication and molecular connection; single-molecule electric characterization; theoretical modeling (PDF)

AUTHOR INFORMATION

Corresponding Authors

Xuefeng Guo − *State Key Laboratory for Structural Chemistry of Unstable and Stable Species, Beijing National Laboratory for Molecular Sciences, National Biomedical Imaging Center, College of Chemistry and Molecular Engineering, Peking University, Beijing 100871, P. R. China; Center of Single-Molecule Sciences, Frontiers Science Center for New Organic Matter, Institute of Modern Optics, College of Electronic Information and Optical Engineering, Nankai University, Tianjin 300350, P. R. China;* orcid.org/0000-0001-5723-8528; Email: guoxf@pku.edu.cn

Hong Guo − *Center for the Physics of Materials and Department of Physics, McGill University, Montreal, Quebec H3A 2T8, Canada*; Email: hong.guo@mcgill.ca

Stéphane Rigaut − *Univ Rennes, CNRS, ISCR (Institut des Sciences Chimiques de Rennes)-UMR 6226, Rennes F-35000, France;* orcid.org/0000-0001-7001-9039; Email: stephane.rigaut@univ-rennes1.fr

Shengxiong Xiao − *The Education Ministry Key Laboratory of Resource Chemistry, Shanghai Key Laboratory of Rare Earth Functional Materials, College of Chemistry and Materials Science, Shanghai Normal University, Shanghai 200234, P. R. China*; Email: xiaosx@shnu.edu.cn

Zhirong Liu − *State Key Laboratory for Structural Chemistry of Unstable and Stable Species, Beijing National Laboratory for Molecular Sciences, National Biomedical Imaging Center, College of Chemistry and Molecular Engineering, Peking University, Beijing 100871, P. R. China;* orcid.org/0000-0001-5070-8048; Email: LiuZhiRong@pku.edu.cn

Authors

Na Xin − *State Key Laboratory for Structural Chemistry of Unstable and Stable Species, Beijing National Laboratory for Molecular Sciences, National Biomedical Imaging Center, College of Chemistry and Molecular Engineering, Peking University, Beijing 100871, P. R. China*

Chen Hu − *Center for the Physics of Materials and Department of Physics, McGill University, Montreal, Quebec H3A 2T8, Canada;* orcid.org/0000-0003-2333-2182

Hassan Al Sabea − *Univ Rennes, CNRS, ISCR (Institut des Sciences Chimiques de Rennes)-UMR 6226, Rennes F-35000, France*

Miao Zhang − *The Education Ministry Key Laboratory of Resource Chemistry, Shanghai Key Laboratory of Rare Earth Functional Materials, College of Chemistry and Materials Science, Shanghai Normal University, Shanghai 200234, P. R. China*

Chenguang Zhou − *State Key Laboratory for Structural Chemistry of Unstable and Stable Species, Beijing National Laboratory for Molecular Sciences, National Biomedical Imaging Center, College of Chemistry and Molecular Engineering, Peking University, Beijing 100871, P. R. China*

Linan Meng − *Institute of Physics, Chinese Academy of Sciences, Beijing 100190, P. R. China*

Chuancheng Jia − *Center of Single-Molecule Sciences, Frontiers Science Center for New Organic Matter, Institute of Modern Optics, College of Electronic Information and Optical Engineering, Nankai University, Tianjin 300350, P. R. China;* orcid.org/0000-0002-1513-8497

Yao Gong − *State Key Laboratory for Structural Chemistry of Unstable and Stable Species, Beijing National Laboratory for Molecular Sciences, National Biomedical Imaging Center, College of Chemistry and Molecular Engineering, Peking University, Beijing 100871, P. R. China*

Yu Li − *State Key Laboratory for Structural Chemistry of Unstable and Stable Species, Beijing National Laboratory for Molecular Sciences, National Biomedical Imaging Center, College of Chemistry and Molecular Engineering, Peking University, Beijing 100871, P. R. China*

Guojun Ke − *State Key Laboratory for Structural Chemistry of Unstable and Stable Species, Beijing National Laboratory for Molecular Sciences, National Biomedical Imaging Center, College of Chemistry and Molecular Engineering, Peking University, Beijing 100871, P. R. China*

Xiaoyan He − *Univ Rennes, CNRS, ISCR (Institut des Sciences Chimiques de Rennes)-UMR 6226, Rennes F-35000, France*

Pramila Selvanathan − *Univ Rennes, CNRS, ISCR (Institut des Sciences Chimiques de Rennes)-UMR 6226, Rennes F-35000, France*

Lucie Norel − *Univ Rennes, CNRS, ISCR (Institut des Sciences Chimiques de Rennes)-UMR 6226, Rennes F-35000, France;* orcid.org/0000-0001-6654-1211

Mark A. Ratner − *Department of Chemistry, Northwestern University, Evanston, Illinois 60208, United States;* orcid.org/0000-0001-7983-3387

Complete contact information is available at: https://pubs.acs.org/10.1021/jacs.1c08997

Author Contributions

[†]N.X., C.H., H.A.S., M.Z. and C.Z. contributed equally.

Funding

This work was financially supported by the National Key R&D Program of China (2017YFA0204901), the National Natural Science Foundation of China (21727806, 21933001, 21772123, and 21773002), the Natural Science Foundation of Beijing (Z181100004418003), Shanghai Engineering Research Center of Green Energy Chemical Engineering (18DZ2254200), the University of Rennes 1, the CNRS and the Agence Nationale de la Recherche (RuOxLux-ANR-12-BS07-0010-01), the Natural Sciences and Engineering Research Council of Canada, the Tencent Foundation through the XPLORER PRIZE and Frontiers Science Center for New Organic Matter at Nankai University (63181206).

Notes

The authors declare no competing financial interest.

■ ACKNOWLEDGMENTS

We thank Abraham Nitzan for the useful discussion, Huimin Wen for helping the characterization of molecular materials, and Hantao Sun and Jianhui Liao for helping the electrical measurement. The authors also thank the High-Performance Computing Centre of McGill University, CalcuQuebec, and Compute Canada for computation facilities, which made the simulations possible.

■ REFERENCES

(1) Xiang, D.; Wang, X.; Jia, C.; Lee, T.; Guo, X. Molecular-Scale Electronics: From Concept to Function. *Chem. Rev.* **2016**, *116*, 4318−4440.

(2) Sun, L.; Diaz-Fernandez, Y. A.; Gschneidtner, T. A.; Westerlund, F.; Lara-Avila, S.; Moth-Poulsen, K. Single-molecule electronics: from chemical design to functional devices. *Chem. Soc. Rev.* **2014**, *43*, 7378−7411.

(3) Xin, N.; Guan, J.; Zhou, C.; Chen, X.; Gu, C.; Li, Y.; Ratner, M. A.; Nitzan, A.; Stoddart, J. F.; Guo, X. Concepts in the design and engineering of single-molecule electronic devices. *Nat. Rev. Phys.* **2019**, *1*, 211−230.

(4) Gehring, P.; Thijssen, J. M.; van der Zant, H. S. J. Single-molecule quantum-transport phenomena in break junctions. *Nat. Rev. Phys.* **2019**, *1*, 381−396.

(5) Zhang, J. L.; Zhong, J. Q.; Lin, J. D.; Hu, W. P.; Wu, K.; Xu, G. Q.; Wee, A. T. S.; Chen, W. Towards single molecule switches. *Chem. Soc. Rev.* **2015**, *44*, 2998−3022.

(6) Han, Y.; Nickle, C.; Zhang, Z.; Astier, H. P. A. G.; Duffin, T. J.; Qi, D.; Wang, Z.; del Barco, E.; Thompson, D.; Nijhuis, C. A. Electric-field-driven dual-functional molecular switches in tunnel junctions. *Nat. Mater.* **2020**, *19*, 843−848.

(7) Zhang, K.; Wang, C.; Zhang, M.; Bai, Z.; Xie, F.-F.; Tan, Y.-Z.; Guo, Y.; Hu, K.-J.; Cao, L.; Zhang, S.; Tu, X.; Pan, D.; Kang, L.; Chen, J.; Wu, P.; Wang, X.; Wang, J.; Liu, J.; Song, Y.; Wang, G.; Song, F.; Ji, W.; Xie, S.-Y.; Shi, S.-F.; Reed, M. A.; Wang, B. A Gd@C_{82} single-molecule electret. *Nat. Nanotechnol.* **2020**, *15*, 1019−1024.

(8) Goswami, S.; Rath, S. P.; Thompson, D.; Hedström, S.; Annamalai, M.; Pramanick, R.; Ilic, B. R.; Sarkar, S.; Hooda, S.; Nijhuis, C. A.; Martin, J.; Williams, R. S.; Goswami, S.; Venkatesan, T. Charge disproportionate molecular redox for discrete memristive and memcapacitive switching. *Nat. Nanotechnol.* **2020**, *15*, 380−389.

(9) Capozzi, B.; Xia, J. L.; Adak, O.; Dell, E. J.; Liu, Z. F.; Taylor, J. C.; Neaton, J. B.; Campos, L. M.; Venkataraman, L. Single-molecule diodes with high rectification ratios through environmental control. *Nat. Nanotechnol.* **2015**, *10*, 522−527.

(10) Chen, X.; Roemer, M.; Yuan, L.; Du, W.; Thompson, D.; del Barco, E.; Nijhuis, C. A. Molecular diodes with rectification ratios exceeding 10^5 driven by electrostatic interactions. *Nat. Nanotechnol.* **2017**, *12*, 797−803.

(11) Perrin, M. L.; Burzuri, E.; van der Zant, H. S. J. Single-molecule transistors. *Chem. Soc. Rev.* **2015**, *44*, 902−919.

(12) Liu, J.; Jiang, L.; Hu, W.; Liu, Y.; Zhu, D. Monolayer organic field-effect transistors. *Sci. China: Chem.* **2019**, *62*, 313−330.

(13) Xin, N.; Guo, X. Catalyst: The Renaissance of Molecular Electronics. *Chem.* **2017**, *3*, 373−376.

(14) 2015 International Technology Roadmap for Semiconductors (ITRS). https://www.semiconductors.org/resources/2015-internationaltechnology-roadmap-for-semiconductor-itrs/ (access date 2021-11-03).

(15) Waldrop, M. M. More than Moore. *Nature* **2016**, *530*, 144−147.

(16) Song, H.; Kim, Y.; Jang, Y. H.; Jeong, H.; Reed, M. A.; Lee, T. Observation of molecular orbital gating. *Nature* **2009**, *462*, 1039−1043.

(17) Xiang, D.; Jeong, H.; Kim, D.; Lee, T.; Cheng, Y.; Wang, Q.; Mayer, D. Three-terminal single-molecule junctions formed by mechanically controllable break junctions with side gating. *Nano Lett.* **2013**, *13*, 2809−2813.

(18) Champagne, A. R.; Pasupathy, A. N.; Ralph, D. C. Mechanically adjustable and electrically gated single-molecule transistors. *Nano Lett.* **2005**, *5*, 305−308.

(19) Bai, J.; Daaoub, A.; Sangtarash, S.; Li, X.; Tang, Y.; Zou, Q.; Sadeghi, H.; Liu, S.; Huang, X.; Tan, Z.; Liu, J.; Yang, Y.; Shi, J.; Meszaros, G.; Chen, W.; Lambert, C.; Hong, W. Anti-resonance features of destructive quantum interference in single-molecule thiophene junctions achieved by electrochemical gating. *Nat. Mater.* **2019**, *18*, 364−369.

(20) Li, Y.; Buerkle, M.; Li, G.; Rostamian, A.; Wang, H.; Wang, Z.; Bowler, D. R.; Miyazaki, T.; Xiang, L.; Asai, Y.; Zhou, G.; Tao, N. Gate controlling of quantum interference and direct observation of anti-resonances in single molecule charge transport. *Nat. Mater.* **2019**, *18*, 357−363.

(21) Zhang, N.; Lo, W. Y.; Cai, Z.; Li, L.; Yu, L. Molecular Rectification Tuned by Through-Space Gating Effect. *Nano Lett.* **2017**, *17*, 308−312.

(22) Perrin, M. L.; Galan, E.; Eelkema, R.; Thijssen, J. M.; Grozema, F.; van der Zant, H. S. A gate-tunable single-molecule diode. *Nanoscale* **2016**, *8*, 8919−8923.

(23) Pathem, B. K.; Claridge, S. A.; Zheng, Y. B.; Weiss, P. S. Molecular switches and motors on surfaces. *Annu. Rev. Phys. Chem.* **2013**, *64*, 605−630.

(24) Irie, M.; Fukaminato, T.; Matsuda, K.; Kobatake, S. Photochromism of diarylethene molecules and crystals: memories, switches, and actuators. *Chem. Rev.* **2014**, *114*, 12174−12277.

(25) Liu, Y.; Lagrost, C.; Costuas, K.; Tchouar, N.; Bozec, H. L.; Rigaut, S. A multifunctional organometallic switch with carbon-rich ruthenium and diarylethene units. *Chem. Commun.* **2008**, 6117−6119.

(26) Jia, C.; Migliore, A.; Xin, N.; Huang, S.; Wang, J.; Yang, Q.; Wang, S.; Chen, H.; Wang, D.; Feng, B.; Liu, Z.; Zhang, G.; Qu, D.-H.; Tian, H.; Ratner, M. A.; Xu, H.; Nitzan, A.; Guo, X. Covalently-bonded single molecule junctions with stable and reversible photoswitched conductivity. *Science* **2016**, *352*, 1443−1445.

(27) Taherinia, D.; Frisbie, C. D. Photoswitchable hopping transport in molecular wires 4 nm in length. *J. Phys. Chem. C* **2016**, *120*, 6442−6449.

(28) Meng, F.; Hervault, Y. M.; Shao, Q.; Hu, B.; Norel, L.; Rigaut, S.; Chen, X. Orthogonally modulated molecular transport junctions for resettable electronic logic gates. *Nat. Commun.* **2014**, *5*, 3023.

(29) Kim, Y.; Hellmuth, T. J.; Sysoiev, D.; Pauly, F.; Pietsch, T.; Wolf, J.; Erbe, A.; Huhn, T.; Groth, U.; Steiner, U. E.; Scheer, E. Charge transport characteristics of diarylethene photoswitching single-molecule junctions. *Nano Lett.* **2012**, *12*, 3736−3742.

(30) Katsonis, N.; Kudernac, T.; Walko, M.; van der Molen, S. J.; van Wees, B. J.; Feringa, B. L. Reversible conductance switching of single diarylethenes on a gold surface. *Adv. Mater.* **2006**, *18*, 1397−1400.

https://doi.org/10.1021/jacs.1c08997
J. Am. Chem. Soc. 2021, 143, 20811−20817

(31) van der Molen, S. J.; Liao, J.; Kudernac, T.; Agustsson, J. S.; Bernard, L.; Calame, M.; van Wees, B. J.; Feringa, B. L.; Schönenberger, C. Light-controlled conductance switching of ordered metal-molecule-metal devices. *Nano Lett.* **2009**, *9*, 76−80.
(32) Arramel; Pijper, T. C.; Kudernac, T.; Katsonis, N.; van der Maas, M.; Feringa, B. L.; van Wees, B. J. Reversible light induced conductance switching of asymmetric diarylethenes on gold: surface and electronic studies. *Nanoscale* **2013**, *5*, 9277−9282.
(33) Xin, N.; Li, X.; Jia, C.; Gong, Y.; Li, M.; Wang, S.; Zhang, G.; Yang, J.; Guo, X. Tuning charge transport in aromatic-ring single-molecule Junctions via ionic-liquid gating. *Angew. Chem., Int. Ed.* **2018**, *57*, 14026−14031.
(34) Xin, N.; Kong, X.; Zhang, Y. P.; Jia, C.; Liu, L.; Gong, Y.; Zhang, W.; Wang, S.; Zhang, G.; Zhang, H. L.; Guo, H.; Guo, X. Control of uipolar/ambipolar transport in single-molecule transistors through interface engineering. *Adv. Electron. Mater.* **2020**, *6*, 1901237.
(35) Aviram, A.; Ratner, M. A. Molecular rectifier. *Chem. Phys. Lett.* **1974**, *29*, 277−283.
(36) Van Dyck, C.; Ratner, M. A. Molecular rectifiers: a new design based on asymmetric anchoring moieties. *Nano Lett.* **2015**, *15*, 1577−1584.
(37) Atesci, H.; Kaliginedi, V.; Celis Gil, J. A.; Ozawa, H.; Thijssen, J. M.; Broekmann, P.; Haga, M. A.; van der Molen, S. J. Humidity-controlled rectification switching in ruthenium-complex molecular junctions. *Nat. Nanotechnol.* **2018**, *13*, 117−121.
(38) Elbing, M.; Ochs, R.; Koentopp, M.; Fischer, M.; von Hänisch, C.; Weigend, F.; Evers, F.; Weber, H. B.; Mayor, M. A single-molecule diode. *Proc. Natl. Acad. Sci. U. S. A.* **2005**, *102*, 8815−8820.
(39) Diez-Perez, I.; Hihath, J.; Lee, Y.; Yu, L.; Adamska, L.; Kozhushner, M. A.; Oleynik, I. I.; Tao, N. Rectification and stability of a single molecular diode with controlled orientation. *Nat. Chem.* **2009**, *1*, 635−641.
(40) Kim, T.; Liu, Z.-F.; Lee, C.; Neaton, J. B.; Venkataraman, L. Charge transport and rectification in molecular junctions formed with carbon-based electrodes. *Proc. Natl. Acad. Sci. U. S. A.* **2014**, *111*, 10928−10932.
(41) Batra, A.; Darancet, P.; Chen, Q.; Meisner, J. S.; Widawsky, J. R.; Neaton, J. B.; Nuckolls, C.; Venkataraman, L. Tuning rectification in single-molecular diodes. *Nano Lett.* **2013**, *13*, 6233−6237.
(42) Kornilovitch, P. E.; Bratkovsky, A. M.; Stanley Williams, R. Current rectification by molecules with asymmetric tunneling barriers. *Phys. Rev. B: Condens. Matter Mater. Phys.* **2002**, *66*, 165436.
(43) Guo, C.; Wang, K.; Zerah-Harush, E.; Hamill, J.; Wang, B.; Dubi, Y.; Xu, B. Molecular rectifier composed of DNA with high rectification ratio enabled by intercalation. *Nat. Chem.* **2016**, *8*, 484−490.
(44) Chen, J.; Kim, M.; Gathiaka, S.; Cho, S. J.; Kundu, S.; Yoon, H. J.; Thuo, M. M. Understanding Keesom interactions in monolayer-based large-area tunneling junctions. *J. Phys. Chem. Lett.* **2018**, *9*, 5078−5085.
(45) Du, C.; Norris, S. R.; Thakur, A.; Chen, J.; VanVeller, B.; Thuo, M. Molecular conformation in charge tunneling across large-area junctions. *J. Am. Chem. Soc.* **2021**, *143*, 13878−13886.
(46) Shimamoto, N.; Ohkoshi, S.; Sato, O.; Hashimoto, K. Control of charge-transfer-induced spin transition temperature on cobalt-iron Prussian blue analogues. *Inorg. Chem.* **2002**, *41*, 678−684.
(47) Li, D.; Clerac, R.; Roubeau, O.; Harte, E.; Mathoniere, C.; Le Bris, R.; Holmes, S. M. Magnetic and optical bistability driven by thermally and photoinduced intramolecular electron transfer in a molecular cobalt−iron Prussian blue analogue. *J. Am. Chem. Soc.* **2008**, *130*, 252−258.
(48) Nihei, M.; Sekine, Y.; Suganami, N.; Nakazawa, K.; Nakao, A.; Nakao, H.; Murakami, Y.; Oshio, H. Controlled intramolecular electron transfers in cyanide-bridged molecular squares by chemical modifications and external stimuli. *J. Am. Chem. Soc.* **2011**, *133*, 3592−3600.

https://doi.org/10.1021/jacs.1c08997
J. Am. Chem. Soc. 2021, 143, 20811−20817